HNPS Advances in Nuclear Physics

Vol 30 (2024)

HNPS2023

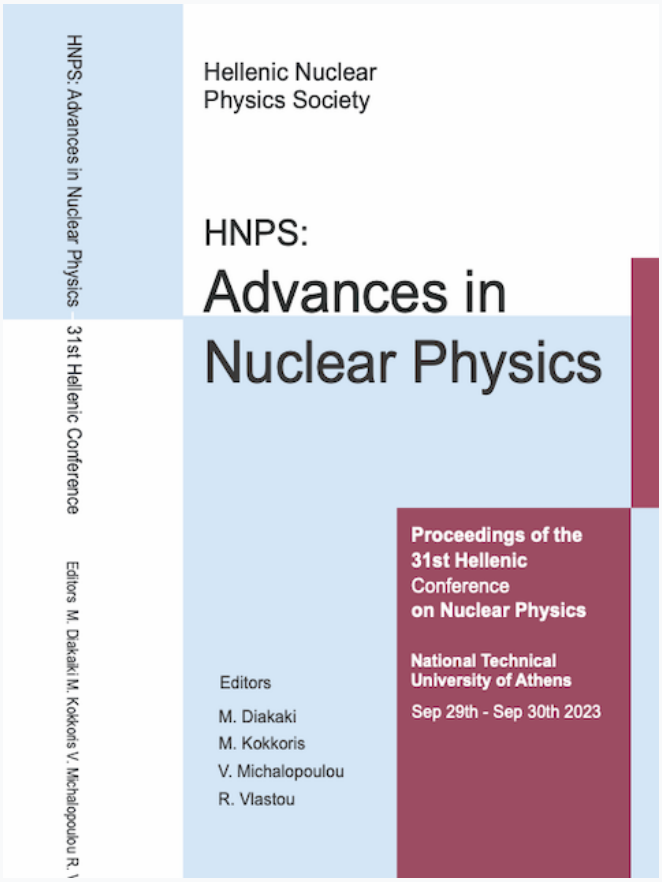

Singlet and Triplet pairing in neutron matter

Eckhard Krotscheck, Jiawei Wang, Panagiota Papakonstantinou

doi: 10.12681/hnpsanp.6153

To cite this article:

Krotscheck, E., Wang, J., & Papakonstantinou, P. (2024). Singlet and Triplet pairing in neutron matter. *HNPS Advances in Nuclear Physics*, *30*, 141–147. https://doi.org/10.12681/hnpsanp.6153

Singlet and Triplet pairing in neutron matter

E. Krotscheck[1,2], P. Papakonstantinou[3], and J. Wang[1]

[1] *Department of Physics, University at Buffalo, SUNY, Buffalo NY 14260, USA*
[2] *Intitut füt Theoretische Physik, Johannes Kepler Universität, A 4040 Linz, Austria*
[3] *Institute for Rare Isotope Science, Institute for Basic Science, Daejeon 34000, Korea*

Abstract The presence of superfluidity in neutron stars can affect the cooling and dynamics of neutron stars in various ways. Model calculations employing realistic nuclear potentials in Bardeen-Cooper-Schrieffer theory generally suggest the development of a $^1S_0$ pairing gap at low densities and a $^3P_2$-$^3F_2$ pairing gap at higher densities. We have evaluated the pairing interaction by summing the "parquet" Feynman diagrams which include both ladder and ring diagrams systematically, *plus* a set of important non-parquet diagrams, making this the most comprehensive diagram-based approach presently available. Our results suggest a modest suppression of the $^1S_0$ pairing gap, a radical suppression of the $^3P_2$-$^3F_2$ triplet pairing gap, and an enhancement of $^3P_0$ pairing.

Keywords Nuclear Astrophysics, Neutron stars, Superfluidity, Neutron Star Cooling

MICROSCOPIC MANY-BODY THEORY

The presence of superfluidity in the various density regimes of a neutron star, from the crust to the inner core, can affect the evolution of neutron stars in various ways. For example, the observed glitches are believed to be caused by the transfer of angular momentum from a neutron superfluid in the inner crust to the rest of the star. The presence or absence of superfluidity in the neutron star interior is also a persistent question in the interpretation of cooling data. The most relevant observation involves the cooling curves of neutron stars, *i.e.*, the evolution of surface temperature with time [1-3]. Superfluidity can induce competing effects: On one hand, it suppresses the direct URCA process. On the other hand, it enhances the pair breaking and formation mechanism when the temperature approaches the critical temperature [2]. More specifically, the comparison of the measured luminosity and inferred temperatures with theoretical predictions reveals the neutrino emissivity, which in turn is affected by superfluidity.

A Nucleon-Nucleon interactions

For the purpose of summing vast arrays of Feynman diagrams, it is most convenient to represent the nucleon-nucleon interaction in an operator basis [4,5] $\hat{v}_n = \sum_{\alpha=1}^{n} \hat{O}_\alpha(i,j)$. Here, $r_{ij} = |r_i - r_j|$ is the distance between particles *i* and *j*, and the $\hat{O}_\alpha(i,j)$ are operators acting on the spin, isospin, and possibly the relative angular momentum variables of the individual particles. Reasonably realistic models for nuclear matter keep at least the six to eight base operators

$$\hat{O}_1(i,j;r_{ij}) \equiv \hat{O}_c = 1\,,$$
$$\hat{O}_3(i,j;\hat{r}_{ij}) \equiv \hat{O}_\sigma(i,j;\hat{r}_{ij}) = \sigma_i{\cdot}\sigma_j\,,$$
$$\hat{O}_5(i,j;\hat{r}_{ij}) \equiv \hat{O}_S(i,j;\hat{r}_{ij}) = 3(\sigma_i\cdot\hat{r}_{ij})(\sigma_j\cdot\hat{r}_{ij}) - \sigma_i{\cdot}\sigma_j\,,$$
$$\hat{O}_7(i,j;\hat{r}_{ij},\hat{p}_{ij}) \equiv \hat{O}_{LS}(i,j;\hat{r}_{ij}) = \hat{r}_{ij}\times\hat{p}_{ij}\cdot S\,,$$

where

$$\hat{O}_{2\alpha}(i,j;\hat{r}_{ij}\{,\hat{p}_{ij}\}) \equiv \hat{O}_{2\alpha-1}(i,j;\hat{r}_{ij}\{,\hat{p}_{ij}\})\tau_i\cdot\tau_j\,.$$

$S = \frac{1}{2}(\sigma_i + \sigma_j)$ is the total spin, and $p_{ij} = \frac{1}{2}(p_i - p_j)$ is the relative momentum operator of the pair of

particles. In neutron matter, the operators are projected to the isospin=1 channel.

B. The case for parquet-diagram summations

Let us begin by making our case that the summation of the so-called class of "parquet" diagrams is the minimum necessary set of Feynman diagrams for a satisfactory description of a strongly interacting system [6]. Fig. 1 shows the schematic equation of state of a self-bound Fermi fluid.

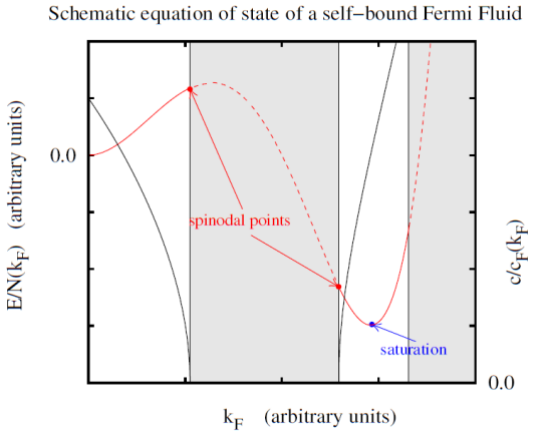

Figure 1. *Schematic equation of state of a self-bound Fermi system (red line) as a function of the Fermi wave number k_F. The red dots indicate the spinodal points, the blue dot the saturation density. The grey-shaded areas depict the density regimes where no homogeneous liquid phase exists. Also shown is the speed of hydrodynamic sound (right scale) which vanishes at the spinodal points. (black line)*

We can typically distinguish four areas:

- At very low densities, the equation of state is dominated by the non-interacting Fermi gas. As the density ρ increases, the attractive interaction begins to become important and the equation of state bends downward until it reaches a "spinodal" point where the hydrodynamic speed of sound $mc^2 = \frac{d}{d\rho}\rho^2 \frac{d}{d\rho}\frac{E}{N}$ vanishes.

- Beyond that spinodal point and up to a density about $2/3$ of the saturation density, no homogeneous phase of the system exists. That regime is depicted as gray-shaded area in Fig. 1 and it ends at a second spinodal point.

- At densities beyond that second spinodal point, the compressibility becomes positive again and the energy per particle has a minimum at the saturation density.

- As the density is further increased, the energy per particle increases again due to the short-ranged repulsion of the interaction. Eventually, the system undergoes a further phase transition for which several scenarios such as quark matter, hyperon matter or kaon condensates have been proposed.

The individual effects –binding, saturation, and excitations like sound propagation– have been studied for a long time. For example, binding and saturation are described, at the simplest level, by the Bethe-Goldstone equation [7], which has been the workhorse of nuclear theory for decades. Likewise, excitations and their stability are described by linear response theory. In the language of perturbation

theory, solving the Bethe-Goldstone equation amounts to summing the "ladder" diagrams. Similarly, the simplest non-trivial implementation of linear response theory, *i.e.*, the "random phase approximation", amounts to summing the "ring" diagrams. Evidently, if one wants both binding and the correct behavior at the spinodal points, one must sum both ring-- and ladder diagrams. This is the aforementioned class of "parquet" diagrams.

C. The case for going beyond parquet-diagram summations

To make the point that the parquet-class misses an important effect for the case of realistic nucleon-nucleon interactions, consider the Goldstone diagrams shown in Fig. 2. The diagram 2a is the ordinary two-body ladder that is summed by the Bethe-Goldstone equation. Parquet-diagram summations supplement the bare interaction by the sum of chain diagrams, an example is shown in diagram 2b. Diagram 2c is by definition not a “parquet” diagram. The interaction matrix elements are basically the same. However, there is a very significant difference:

Consider a pair of particles $(k_1\sigma_1, k_2\sigma_2)$ entering one of the processes shown in Fig. 2. If these particles are in a spin-singlet state, they will remain in that state throughout the processes shown in Fig. 2a and 2b. In the process shown in Fig. 2c, the chain depicted by the two wavy lines can also carry a spin; spin-conservation therefore implies that the bare interaction line is a triplet interaction. Therefore, the spin-triplet interaction will contribute to the spin-singlet component of the *G*-matrix. Similarly, the spin-singlet interaction contributes to the spin-triplet component of the *G*-matrix. Since the spin-triplet interaction is repulsive, one should expect a reduced attraction in the spin-singlet *G*-matrix and, vice versa, a somewhat more attractive spin-triplet *G*-matrix.

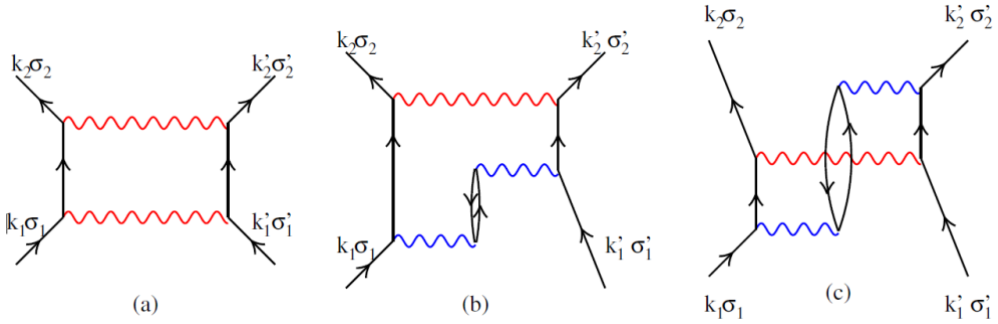

Figure 2. *The simplest second-order ladder diagrams including a "twisted chain" correction. The middle diagram is where one of the bare interactions is replaced by the “induced interaction” $w_I(q)$, and the right one is the simplest contribution to the totally irreducible interaction. The red wavy line represents the bare interaction and the blue wavy line the particle-hole interaction. The chains of two blue wavy lines may, of course, be supplemented by longer chains.*

RESULTS: PAIRING PHENOMENA

A. Theory

The superfluid phase transition in neutron matter has been studied for decades; see, for example, Refs. [8] and [9] for recent reviews and extensive compilations of the relevant literature. We can basically distinguish four types of calculations:

- Calculation of the superfluid gap at the mean-field level using bare, more or less realistic nuclear interactions. See for example Refs. [10] and [11].

- Medium polarization effects can have a profound influence on superfluid transition temperature

[12-15]. The presently most sophisticated treatment of these effects is found in Ref. [16]. That work also came to the conclusion that the effect of polarization can be quite dramatic. To calculate polarization corrections, assumptions on the quasiparticle interaction must be made.

- The inclusion of many-body effects may be traced to a formulation of correlated basis function theory [17] superfluid systems [18,19] or extensions of Brueckner-Bethe-Goldstone theory [20-22]. Generally, the method can be mapped onto a regular BCS-like theory with effective interactions, the essential task then being the calculation of these effective interactions with a trustworthy accuracy.

- Some Monte Carlo calculations exist for *S*-wave pairing in low-density neutron matter [23]. Our results of Ref. [24] agree quite well with these calculations; whether the extension of Monte Carlo methods for systems where complicated tensor- and spin-orbit components of the interaction are essential, remains to be seen.

In the above classification of methods, our work belongs to the third category. We calculate the pairing interaction by a self-consistent summation of all ring- and ladder-diagrams which corresponds, in the language of Jastrow-Feenberg theory, to the optimized Fermi-Hypernetted-Chain (FHNC-EL) summation method. We also include the non-parquet diagrams discussed in section 1.C.

B. S-wave pairing

The simplest case is *S*-wave pairing. We have performed calculations for the Reid and Argonne interactions; the results are rather similar and we show, therefore, only those for the v_8 version of the Argonne potential. Fig. 3 shows a sequence of results: The pairing gap as calculated by using the bare interaction, the result including short-ranged correlations and polarization corrections (labeled as "parquet") and those obtained by including the "beyond parquet" corrections (labeled as "twisted chains"). As it is seen, correlations reduce the gap by about 60 percent and the inclusion of "twisted chain" corrections by another 50 percent. The latter then brings us in close proximity to QMC calculations [23], although the comparison must be taken with caution, see the discussion in Ref. [24].

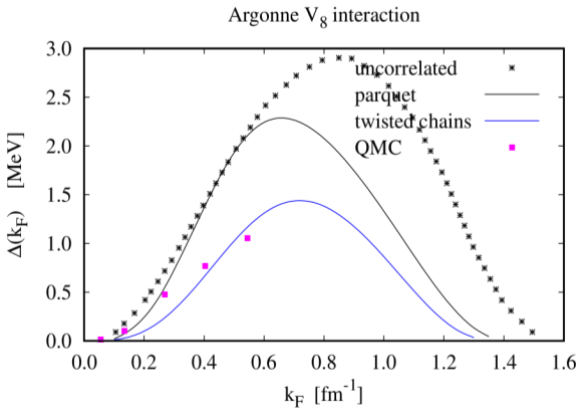

***Figure 3**: Superfluid gap Δ(k_F) for $^1S_0$ pairing at the Fermi momentum for the Argonne v_8 interaction. We show the parquet calculation (black curve) and the "beyond parquet" results. The crosses show the results for the bare interaction [11,26]. The magenta squares are quantum Monte Carlo data from Ref. [23].*

C. P-wave pairing

The study of *P*-wave paring was initiated by the pioneering work of Tamagaki *et al.* [27,28] who concluded that $^3P_2$ and $^3P_2$-$^3F_2$ pairing prevails in neutron star matter, but there is no significant pairing in $^3P_0$ states. These calculations were based on interactions that reproduced reasonably well the *P*-wave scattering data.

However, when all the many-body effects described above are taken into account, the situation changes drastically. The two channels of *P*-wave pairing are reversed; in particular, $^3P_2$-$^3F_2$ pairing becomes minute whereas we have a sizable $^3P_0$ gap, see Fig. 4.

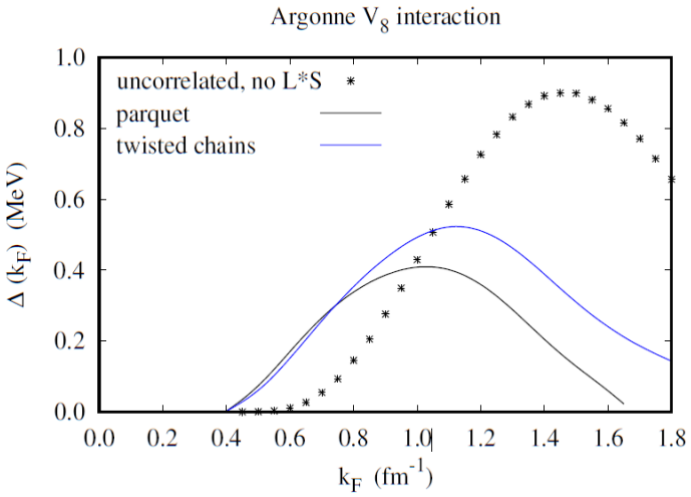

Figure 4: *Superfluid gap $\Delta(k_F)$ for $^3P_0$ pairing at the Fermi momentum for the Argonne v_8 interaction. We show the parquet calculation (black curve) and the "beyond parquet" results. The crosses show the results for the bare interaction [26] when the spin-orbit force has been turned off.*

The reason for this reversal is our result [29] that the spin-orbit potential is strongly suppressed by many-body correlations. The special role of the spin-orbit interaction has been pointed out in Ref. [30]: "without an attractive spin-orbit interaction, neutrons would form a $^3P_0$ superfluid, in which the spin and orbital angular momenta are anti-aligned, rather than the $^3P_2$ state, in which they are aligned." This statement is, of course, based on properties of the bare interaction.

While the effect we are pointing out here seems to be an intricate consequence of high-level microscopic many-body theory, it is actually quite plausible as soon as one goes beyond mean-field pictures: The reason for nuclear saturation is the strong short-ranged repulsion that keeps the nucleons apart from each other. The effect is manifested in the *pair distribution function* $g(r)$ which is a normalized probability to find a pair of particles at a certain distance. Fig. 5 shows the function $g_T(r)$ for a pair of neutrons with parallel spin along with the bare central and spin-orbit interaction. Evidently, short-ranged screening has the effect that two neutrons never come close enough to each other so that they can "see" the attractive spin-orbit force. Thus, high-level many-body theory as utilized here is necessary for the *quantitative* determination of the screening effect, the effect is *qualitatively* quite plausible.

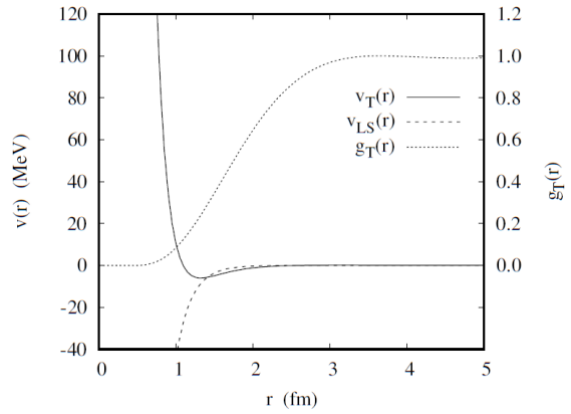

Figure 5. *The figure shows the interaction of a pair of neutrons in a spin-triplet state (solid line), the resulting spin-triplet pair distribution function* $g_T(r)$ *(short-dashed line) and the spin-orbit potential (long-dashed line)*

CONCLUSIONS

With the present results we have challenged an over 50 years old narrative initiated by the pioneering work of Tamagaki *et al*. [27,28] that $^3P_2$ and $^3P_2$-$^3F_2$ pairing prevails in neutron star matter. The reason for this reversal is our result [29] that the spin-orbit potential is strongly suppressed by many-body correlations. There are a number of obvious ways of extending our calculations. One of them is the inclusion of three-nucleon forces, whose combined effect with in-medium mass normalization can vary strongly depending on the adopted approach. Another possible extension is to use a superfluid Lindhard function for the calculation of the induced interaction, whose effect can be quite large in low-density neutron matter where the gap can be as large as half of the Fermi energy.

Acknowledgments

This work was supported, in part, by the College of Arts and Sciences of the University at Buffalo, SUNY (to J.W.). Participation of EK at this conference was supported by a grant from the president's office, SUNY Buffalo. P.P. was supported by the Rare Isotope Science Project of the Institute for Basic Science funded by the Ministry of Science, ICT and Future Planning and the National Research Foundation (NRF) of Korea (2013M7A1A1075764).

References

[1] D. Page and S. Reddy, Ann. Rev. Nucl. Part. Sci. 56, 327 (2006)
[2] D. Page et al., in *Novel Superfluids*, Vol. 2, edited by K.-H. Bennemann and J.B. Ketterson (Oxford University Press, Oxford, UK, 2015) Chap. 21, pp. 505-579
[3] D.G. Yakovlev and P. Haensel, Astronomy and Astrophysics 407, 259 (2003)
[4] B.D. Day, Phys. Rev. C 24, 1203 (1981)
[5] R.B. Wiringa, V.G.J. Stoks, and R. Schiavilla, Phys. Rev. C 51, 38 (1995)
[6] A.D. Jackson and T. Wettig, Phys. Rep. 237, 1 (1993)
[7] H.A. Bethe and J. Goldstone, Proc. R. Soc. London, Ser. A 238, 551 (1957)
[8] A. Sedrakian and J.W. Clark, EPJ A 55, 167 (2019)
[9] G.C. Strinati et al., Phys. Rep. 738, 1 (2018)
[10] M. Baldo et al., Phys. Rev. C 58, 192 (1998)
[11] V.A. Khodel, V.V. Khodel, and J.W. Clark, Nucl. Phys. A 598, 390 (1996)
[12] J.W. Clark et al., Phys. Lett. B 61, 331 (1976)
[13] J.M.C. Chen et al., Nucl. Phys. A 555, 59 (1993)
[14] J. Wambach, T. Ainsworth, and D. Pines, Nucl. Phys. A 555, 128 (1993)
[15] H.-J. Schulze et al., Phys. Lett. B 375, 1 (1996)
[16] A. Schwenk and B. Friman, Phys. Rev. Lett. 92, 082501 (2004)
[17] E. Feenberg, Theory of Quantum Fluids (Academic Press, New York, 1969)
[18] E. Krotscheck and J.W. Clark, Nucl. Phys. A 333, 77 (1980)
[19] S. Fantoni, Nucl. Phys. A 363, 381 (1981)

[20] H.-J. Schulze, A. Polls, and A. Ramos, Phys. Rev. C 63, 044310 (2001)
[21] D. Ding et al., Phys. Rev. C 94, 025802 (2016)
[22] A. Rios, A. Polls, and W. H. Dickhoff, J. Low Temp. Phys. 189, 234 (2017)
[23] A. Gezerlis and J. Carlson, Phys. Rev. C 77, 032801(R) (2008)
[24] E. Krotscheck and J. Wang, Phys. Rev. C 103, 035808 (2021)
[25] T. Takatsuka and R. Tamagaki, Progress of Theoretical Physics 46, 114 (1971)
[26] E. Krotscheck et al., Phys. Rev. C 109, 015803 (2024)
[27] R. Tamagaki, Prog. Theor. Phys. 44, 905 (1970)
[28] T. Takatsuka, Progress of Theoretical Physics 48, 1517 (1972)
[29] E. Krotscheck and J. Wang, Phys. Rev. C 105, 034345 (2022)
[30] A. Gezerlis, C. J. Pethick, and A. Schwenk, in Novel Superfluids, Vol. 2, edited by K.H. Bennemann and J.B. Ketterson (Oxford University Press, 2014) Chap. 22, pp. 580-615